

Interplay between edge and bulk states in silicene nanoribbon

Xing-Tao An,^{1,2,*} Yan-Yang Zhang,^{2,3} Jian-Jun Liu,⁴ and Shu-Shen Li²

¹*School of Sciences, Hebei University of Science and Technology, Shijiazhuang, Hebei 050018, China*

²*SKLSM, Institute of Semiconductors, Chinese Academy of Sciences, P. O. Box 912, Beijing 100083, China*

³*International Center for Quantum Materials, Peking University, Beijing 100871, China*

⁴*Physics Department, Shijiazhuang University, Shijiazhuang 050035, China*

(Dated: June 5, 2022)

We investigate the interplay between the edge and bulk states, induced by the Rashba spin-orbit coupling, in a zigzag silicene nanoribbon in the presence of an external electric field. The interplay can be divided into two kinds, one is the interplay between the edge and bulk states with opposite velocities, and the other is that with the same velocity direction. The former can open small direct spin-dependent subgaps. A spin-polarized current can be generated in the nanoribbon as the Fermi energy is in the subgaps. While the later can give rise to the spin precession in the nanoribbon. Therefore, the zigzag silicene nanoribbon can be used as an efficient spin filter and spin modulation device.

PACS numbers: 75.76.+j; 72.80.Vp; 73.21.b

Graphene, a two-dimensional honeycomb network of carbon atoms, has received great attention in recent years due to its unique physical properties and application potentials in future nanoelectronic devices.[1–3] The discovery of graphene forms a platform to explore the properties of two-dimensional honeycomb electronic systems. However, its compatibility with current silicon-based nanotechnologies may face challenges. Recently, strong effort has been invested to search theoretically and experimentally for two-dimensional honeycomb structures formed by other elements, such as silicon.[4–17] Silicene, a sheet of silicon atoms forming a honeycomb lattice analogous to graphene, has been theoretically predicted and successfully synthesized.[4–8] Many striking electric properties of graphene, such as zero gap, linear dispersion of the electron band and high Fermi velocity, could be transferred to silicene.

Different from graphene, silicene has a buckled structure owing to a large ionic radius of silicon, which creates new possibilities for manipulating the dispersion of electrons and controlling band gap electrically in silicene.[9] Furthermore, silicene has a relatively large spin-orbit gap of 1.55meV that may induce quantum spin Hall effect and quantum anomalous Hall effect.[7, 11] A topological phase transition from a quantum spin Hall state to a band insulator can be induced by an external electric field in silicene.[10] A valley polarized quantum Hall effect has also been demonstrated in the presence of a perpendicular external magnetic field.[11] The extraordinary transport properties of silicene nanoribbons have also been studied theoretically. For example, Kang et al., using first principles calculations, studied the symmetry-dependent transport properties and magnetoresistance effect in silicene nanoribbons.[12] The spin-polarized current induced by a local exchange field in a silicene nanoribbon has been investigated in our previous work.[13]

In this Letter, we study the interplay between the edge and bulk states induced by the Rashba spin-orbit coupling in the zigzag silicene nanoribbon in the presence of an external electric field, by using the nonequilibrium Green's function method. Due to the effective spin-orbit coupling and the staggered sublattice potential induced by an external electric field, the spin polarization in silicene is opposite at different valleys, which is called the valley-spin locking.[10] The interplay between the edge and bulk states occurs when the Rashba spin-orbit coupling exists in the silicene nanoribbon. Different from subband mixing due to the spin-orbit coupling in the conventional semiconductor quantum wires,[18–24] the interplay between the edge and bulk states with opposite group velocity opens a small, direct and spin-dependent subgap. At a given Fermi level in this subgap, an obvious spin polarized current can be obtained because of the disequilibrium of spin-up and spin-down states with positive group velocities (i.e., right going channels).

The silicene system with an external electric field is described by the the following Hamiltonian:[14]

$$\begin{aligned} H = & -t \sum_{\langle ij \rangle \alpha} c_{i\alpha}^\dagger c_{j\alpha} + i \frac{\lambda_{SO}}{3\sqrt{3}} \sum_{\langle\langle ij \rangle\rangle \alpha\beta} \nu_{ij} c_{i\alpha}^\dagger \sigma_{\alpha\beta}^z c_{j\beta} \\ & - i \frac{2}{3} \lambda_R \sum_{\langle\langle ij \rangle\rangle \alpha\beta} \mu_i c_{i\alpha}^\dagger (\boldsymbol{\sigma} \times \mathbf{d}_{ij}^0)_{\alpha\beta}^z c_{j\beta} \\ & + \lambda_\nu \sum_{i\alpha} \mu_i c_{i\alpha}^\dagger c_{i\alpha}, \end{aligned} \quad (1)$$

where $c_{i\alpha}^\dagger$ creates an electron with spin polarization α at site i ; $\langle ij \rangle$ and $\langle\langle ij \rangle\rangle$ run over all the nearest and next-nearest neighbor hopping sites, respectively. The first term is the nearest-neighbor hopping with the transfer energy $t = 1.6\text{eV}$. The second term describes the effective spin-orbit coupling, where $\boldsymbol{\sigma} = (\sigma_x, \sigma_y, \sigma_z)$ is the Pauli matrix of spin and ν_{ij} is defined as $\nu_{ij} = (\mathbf{d}_i \times \mathbf{d}_j)/|\mathbf{d}_i \times \mathbf{d}_j| = \pm 1$ with \mathbf{d}_i and \mathbf{d}_j the two bonds

connecting the next-nearest neighbors \mathbf{d}_{ij} . The third term represents the Rashba spin-orbit coupling, where $\mu_i = \pm 1$ for the A (B) site, and $\mathbf{d}_{ij}^0 = \mathbf{d}_{ij}/|\mathbf{d}_{ij}|$. The fourth term is a staggered sublattice potential and its strength λ_ν can be tuned by a perpendicular electric field due to the buckling distance between two sublattices of the silicene.

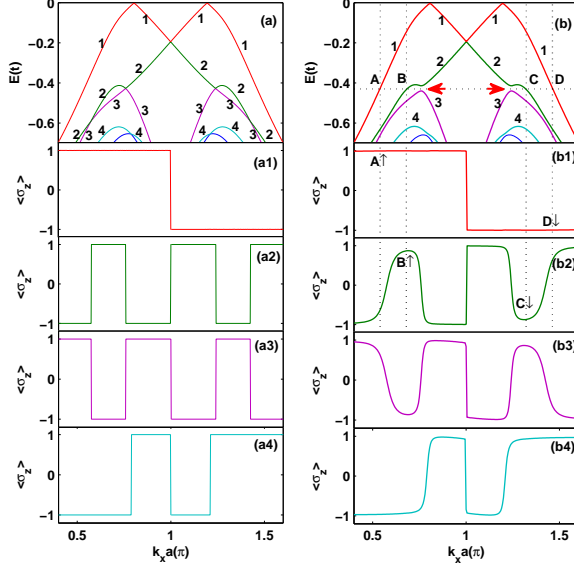


FIG. 1: (color online) The energy spectrum (a), (b) and the corresponding spectrum of the spin $\langle \sigma_z \rangle$ (a1-a4) and (b1-b4) of a zigzag silicene nanoribbon for $\lambda_R = 0$ (a) and $\lambda_R = 0.07t$ (b). The numbers in (a) and (b) denote the different states. At a given Fermi level in the subgap there exist four different states, which are labeled as A, B, C, and D, in which \uparrow (\downarrow) stands for the up (down) spin polarization. The horizontal arrows in (b) point to the small subgaps in the energy spectrum.

In order to assure the system in the quantum spin Hall state, we set the parameters $\lambda_{SO} = 0.3t$ and $\lambda_\nu = 0.2t$. [10, 11] The length of the zigzag silicene nanoribbon L is taken to be infinite. The energy spectrum of the zigzag silicene nanoribbon, together with the corresponding eigenfunctions $\varphi_n(k_x)$, can be numerically obtained by diagonalizing the Hamiltonian for each momentum k_x in the x direction. [25] The calculated energy spectrum of the zigzag silicene nanoribbon with width $W = 14a/\sqrt{3}$ ($N_y = 20$), where a is the next nearest-neighbor distance, for $\lambda_R = 0$ and $\lambda_R = 0.07t$ is plotted in Figs. 1(a) and (b), respectively. Edge states appear in the bulk band gap of the energy spectrum whether there exists Rashba spin-orbit coupling or not, since this small λ_R does not lead to a topological phase transition.

Let's focus on the top of the bulk valence band, where it meets the edge states, i.e., subbands labeled as 2 and 3 in Figs. 1(a) and (b). Without Rashba spin-orbit cou-

pling (Fig. 1(a)), the edge states cross with the bulk valley with opposite spin, [11] as can be seen in Figs. 1(a2) and (a3). In this case, there is no interplay between them due to the absence of spin-flip effects. Finite λ_R , on the other hand, couples these two subbands and leads to anti-crossings between them as seen in Fig. 1(b). There are two cases for interplays between the edge and bulk subbands (channels). The first case (anti-parallel crossing) happens at the energy $E \sim -0.43t$ near the Dirac point, between the states with opposite group velocities v ($v = 1/\hbar(\partial E/\partial k_x)$). The second case (parallel crossing), however, corresponds to the crossing between states with the same direction of velocity, at the energy $E \sim -0.6t$. Notice that the subgap opened by the Rashba spin-orbit coupling is direct (indirect) for the anti-parallel (parallel) crossing, respectively. This is the essential physics we will rely on in this work.

We also calculate the k_x -dependent expectation value of spin, $\langle \sigma_z \rangle = \langle \varphi_n(k_x) | \sigma_z | \varphi_n(k_x) \rangle$ for the n th occupied states. The calculated $\langle \sigma_z \rangle$ for the same parameters as in Figs. 1(a) and 1(b) are shown in Figs. 1(a1-a4) and (b1-b4), in which the color of the line denotes different states. We can see from Figs. 1(a1) and (b1) that the Dirac cone around K (K') point is polarized with spin up (down) due to the effective spin-orbit coupling and the external electric field for the system with or without Rashba spin-orbit coupling. If $\lambda_R = 0$, σ_z and the Hamiltonian H commute. Therefore, σ_z is a good quantum number, and the expectation value of spin $\langle \sigma_z \rangle$ consists of just two values ± 1 , as shown in Figs. 1(a1-a4). When the Rashba term is turned on, σ_z no longer commutes with the Hamiltonian H . In this case, a continuous variation between $+1$ and -1 in spin polarization of the states with k_x appear.

At a given Fermi level in the direct subgap opened by the Rashba spin-orbit coupling, there exist four different states labeled as A, B, C, and D. From Fig. 1(b), one can easily find that the electrons in states A and B are right-going waves with velocity in the positive x direction, while the electrons in states C and D are left-going waves with velocity in the negative x direction. We can also examine the spin polarization of the states from Figs. 1(b1) and (b2), states A and B being almost fully spin-up polarized and states C and D spin-down polarized. Therefore, under a definite arrangement of bias voltage, there remains only the right-going channel with spin-up electrons, that is, a spin-polarized current appears in the system as the Fermi level is in the direct subgaps opened by the Rashba spin-orbit coupling.

In order to investigate this spin polarization in a more direct way, we calculate the spin-dependent conductance and spin polarization using the nonequilibrium Green's function method. The following discussion is based on the assumption that only the nearest-neighbor hopping exists in the left and right leads, i.e., the Hamiltonian of lead- p is simply $H_p = -t \sum_{\langle ij \rangle \alpha} c_{i\alpha}^\dagger c_{j\alpha}$. The conductance

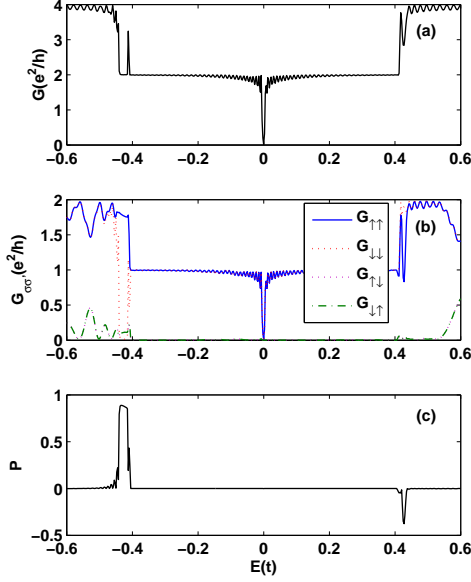


FIG. 2: (Color online) The total conductance G (a), spin-dependent conductance $G_{\sigma\sigma'}$ (b) and spin polarization P (c) of the zigzag silicene nanoribbon vs E for $\lambda_R = 0.07t$.

matrix is calculated by Landauer formula[26]

$$G = \begin{pmatrix} G_{\uparrow\uparrow} & G_{\uparrow\downarrow} \\ G_{\downarrow\uparrow} & G_{\downarrow\downarrow} \end{pmatrix} = \frac{e^2}{h} \sum_{i,j=1}^{N_y} \begin{pmatrix} |t_{ij,\uparrow\uparrow}|^2 & |t_{ij,\uparrow\downarrow}|^2 \\ |t_{ij,\downarrow\uparrow}|^2 & |t_{ij,\downarrow\downarrow}|^2 \end{pmatrix}. \quad (2)$$

The transmission matrix is $t = 2\sqrt{\Gamma_L}G_{1N_x}^r\sqrt{\Gamma_R}$, where $\Gamma_p(E) = i[\Sigma_p^r(E) - \Sigma_p^a(E)]$ is the line-width function with a well-defined matrix square root and $G_{1N_x}^r$ that connects the unit cells 1 and N_x along the direction of transport is the $4N_y \times 4N_y$ submatrix of the full Green function matrix. The retarded (advanced) self-energy Σ_p^r ($\Sigma_p^a = [\Sigma_p^r]^\dagger$) describing the interaction of the sample with the lead- p can be calculated numerically.[27] The total conductance G and the spin polarization P in lead- R can be respectively defined as

$$G = G_{\uparrow\uparrow} + G_{\downarrow\uparrow} + G_{\uparrow\downarrow} + G_{\downarrow\downarrow} \quad (3)$$

and

$$P = \frac{G_{\uparrow\uparrow} + G_{\downarrow\uparrow} - G_{\uparrow\downarrow} - G_{\downarrow\downarrow}}{G_{\uparrow\uparrow} + G_{\downarrow\uparrow} + G_{\uparrow\downarrow} + G_{\downarrow\downarrow}}. \quad (4)$$

We assume that the length of the zigzag silicene nanoribbon is $L = 100a$ ($N_x=100$). Figs. 2(a), (b) and (c) show the total conductance, spin-dependent conductance and spin polarization versus energy E for $\lambda_R = 0.07t$, respectively. In Fig. 2(a), the plateau like structure of the total conductance in units of $2e^2/h$ is observed immediately. However, the resonance like structure is superimposed on the conductance plateau because of the

mismatch between the central sample and the leads. Due to the finite size effect, the edge states of the sample are coupled with each other and a small gap in the energy spectrum of the edge states is opened, so a narrow dip emerges in the conductance at $E = 0$. From Fig. 2(b) we can find that the spin-up and spin-down electrons are not mixed i.e., $G_{\uparrow\downarrow} = G_{\downarrow\uparrow} = 0$ when the energy E is in the bulk gap because there are only edge states protected by topological invariants in the bulk gap. When the energy E is in the bulk band, the interplay between the edge and bulk states induced by the Rashba spin-orbit coupling can lead to the spin precession. Therefore in this case, $G_{\uparrow\downarrow} = G_{\downarrow\uparrow} \neq 0$. It is more interesting that as the energy E is in the direct subgaps opened by the Rashba spin-orbit coupling, $G_{\uparrow\uparrow}$ is very large while $G_{\downarrow\downarrow}$ is almost equal to zero because the electrons traveling from left to right in the zigzag silicene nanoribbon are almost spin up. Therefore, the spin polarization can be very large when the energy is in the direct subgaps opened by the Rashba spin-orbit coupling, as shown in Fig. 2(c). The spin polarization can be also obtained at $E \sim 0.43t$ due to the interplay between the edge and conduction subbands. However, the value of the spin polarization is smaller than that at $E \sim -0.43t$ because the electron-hole symmetry is broken by the Rashba spin-orbit coupling.

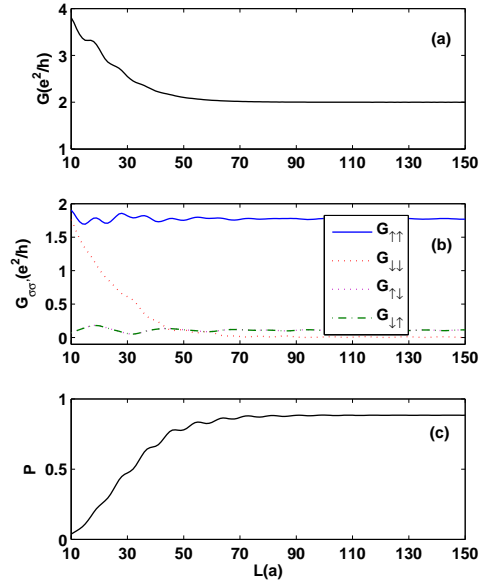


FIG. 3: (Color online) The total conductance G (a), spin-dependent conductance $G_{\sigma\sigma'}$ (b) and spin polarization P (c) vs the length L of the zigzag silicene nanoribbon for $\lambda_R = 0.07t$ and $E = -0.43t$.

In Fig. 3, we show the total conductance G , spin-dependent conductance $G_{\sigma\sigma'}$ and spin polarization P versus the length of the zigzag silicene nanoribbon L for

$E = -0.43t$ which is in the direct subgaps opened by the Rashba spin-orbit coupling. This case corresponds to the interplay between the traveling edge and bulk states with the opposite velocity. When the length of the nanoribbon is very short, for example $L = 10a$, the band structure as shown in Fig. 1(b) has not been formed well and the electrons quickly tunnel through the sample. As the length of the nanoribbon increases to $50a$, the total conductance becomes $2e^2/h$ and the conductance $G_{\downarrow\downarrow}$ becomes zero because there are only two spin-up modes involved in transport and the spin-down electrons are reflected back to the left lead. Therefore, for the energy in the direct subgaps opened by the Rashba spin-orbit coupling, the spin polarization can reach a very large value as the length of the nanoribbon increases, as shown in Fig. 3(c).

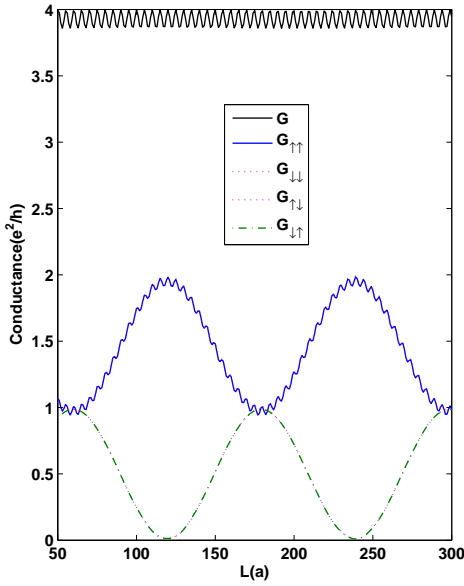


FIG. 4: (Color online) The total conductance G , spin-dependent conductance $G_{\sigma\sigma'}$ and spin polarization P vs the length L of the zigzag silicene nanoribbon for $\lambda_R = 0.07t$ and $E = -0.6t$.

Fig. 4 shows the total conductance G and spin-dependent conductance $G_{\sigma\sigma'}$ versus the length of the zigzag silicene nanoribbon L for $E = -0.6t$, which correspond to the “parallel crossing”, i.e., interplay between the traveling edge and bulk states with the same direction of velocities. The largest value of the total conductance is $4e^2/h$ because there are four spin-dependent modes, including a spin-up mode, a spin-down mode, and two spin-mixing modes, at the Fermi energy contributing to the conductance. Due to the mismatch between the sample and the leads, the total conductance shows resonant transmission properties. From Fig. 4 we can see that $G_{\uparrow\uparrow} = G_{\downarrow\downarrow}$ and $G_{\uparrow\downarrow} = G_{\downarrow\uparrow}$, so the spin po-

larization can not occur at the energy. However, all of the spin-dependent conductances vary periodically as the length of the zigzag silicene nanoribbon L varies. This periodical variation of the spin-dependent conductances originates from the spin mixing induced by the interplay between the traveling edge and bulk states with the same velocity. Due to the Rashba spin-orbit coupling, the spin precesses in the nanoribbon at the energy. As the length gradually increases, the amount of spin rolling from left to right will change periodically. Therefore, the perfect spin modulation of conductance occurs in the situation of parallel crossing.

Before arriving at the final summary, we emphasize that the above phenomena are not a simple finite-size effect. With increasing transverse size, there will be more bulk channels crossing the edge channels, therefore there will be many parallel crossings (showing periodic and spin-dependent conductances) and anti-parallel crossings (showing spin polarization).

In summary, we study the interplay of the edge and bulk states induced by the Rashba spin-orbit coupling in a zigzag silicene nanoribbon in the presence of an external electric field. We find that the interplay can be classified two types: (i) anti-parallel crossing, the interplay between the edge and bulk states with opposite velocities, which opens small and direct spin-dependent subgaps; (ii) parallel crossing, the interplay between the edge and bulk states with same velocity direction, which gives rise to the significant anticrossing of the subbands. The spin-dependent transport properties of the zigzag silicene nanoribbon are also investigated by using nonequilibrium Green’s function method. For the former, a spin-polarized current in the nanoribbon can be generated as the Fermi energy is in the direct spin-dependent subgaps. While the later can give rise to the spin precession in the nanoribbon. The interplay of the edge and bulk states induced by the Rashba spin-orbit coupling in the zigzag silicene nanoribbon is different from that of subbands in conventional semiconductor nanoribbon, in which the Rashba spin-orbit coupling can only gives rise to the spin precession.

This work was supported by National Natural Science Foundation of China (Grant Nos. 11104059 and 61176089), Hebei province Natural Science Foundation of China (Grant No. A2011208010), and Postdoctoral Science Foundation of China (Grant No. 2012M510523).

* Electronic address: anxingtiao@semi.ac.cn

- [1] K. S. Novoselov, A. K. Geim, S. V. Morozov, D. Jiang, Y. Zhang, S. V. Dubonos, I. V. Grigorieva, and A. A. Firsov, *Science* **306**, 666 (2004).
- [2] A. K. Geim, *Science* **324**, 1530 (2009).
- [3] S. Das Sarma, Shaffique Adam, E. H. Hwang, and Enrico Rossi, *Rev. Mod. Phys.* **83**, 407 (2011).

- [4] P. De Padova, C. Quaresima, C. Ottaviani, P. M. Sheverdyayeva, P. Moras, C. Carbone, D. Topwal, B. Olivieri, A. Kara, H. Oughaddou, B. Aufray, and G. Le Lay, *Appl. Phys. Lett.* **96**, 261905 (2010).
- [5] M. Houssa, G. Pourtois, V. V. Afanasev, and A. Stesmans, *Appl. Phys. Lett.* **97**, 112106 (2010).
- [6] B. Lalmi, H. Oughaddou, H. Enriquez, A. Kara, S. Vizzini, B. Ealet, and B. Aufray, *Appl. Phys. Lett.* **97**, 223109 (2010).
- [7] C.-C. Liu, W. Feng, and Y. Yao, *Phys. Rev. Lett.* **107**, 076802 (2011).
- [8] P. Vogt, P. De Padova, C. Quaresima, J. Avila, E. Frantzeskakis, M. C. Asensio, A. Resta, B. Ealet, and G. Le Lay, *Phys. Rev. Lett.* **108**, 155501 (2012).
- [9] N. D. Drummond, V. Zolyomi, and V. I. Fal'ko, *Phys. Rev. B* **85**, 075423 (2012).
- [10] M. Ezawa, *New J. Phys.* **14**, 033003 (2012).
- [11] M. Ezawa, *Phys. Rev. Lett.* **109**, 055502 (2012).
- [12] J. Kang, F. Wu, and J. Li, *Appl. Phys. Lett.* **100**, 233122 (2012).
- [13] X. T. An, Y. Y. Zhang, J. J. Liu, and S. S. Li, *New J. Phys.* **14**, 083039 (2012).
- [14] C. C. Liu, H. Jiang, Y. G. Yao, *Phys. Rev. B* **84**, 195430 (2011).
- [15] M. Tahir and U. Schwingenschlögl, *Appl. Phys. Lett.* **101**, 132412 (2012).
- [16] X. T. An, Y. Y. Zhang, J. J. Liu, and S. S. Li, *Appl. Phys. Lett.* **102**, 043113 (2013).
- [17] L. Chen, H. Li, B. Feng, Z. Ding, J. Qiu, P. Cheng, K. Wu, and S. Meng, *Phys. Rev. Lett.* **110**, 085504 (2013).
- [18] X. F. Wang and P. Vasilopoulos, *Phys. Rev. B* **68**, 035305 (2003).
- [19] A. V. Moroz and C. H. W. Barnes, *Phys. Rev. B* **60**, 14272 (1999).
- [20] F. Mireles and G. Kirczenow, *Phys. Rev. B* **64**, 024426 (2001).
- [21] X. F. Wang, *Phys. Rev. B* **69**, 035302 (2004).
- [22] H. Su, B.-Y. Gu, *Phys. Lett. A* **335**, 316 (2005).
- [23] Q.-F. Sun and X. C. Xie, *Phys. Rev. B* **71**, 155321 (2005).
- [24] S. Zhang, R. Liang, E. Zhang, L. Zhang, and Y. Liu, *Phys. Rev. B* **73**, 155316 (2006).
- [25] H. Li, L. Sheng, and D. Y. Xing, *Phys. Rev. Lett.* **108**, 196806 (2012).
- [26] M. Kariminezhad and A. Namiranian, *J. Appl. Phys.* **110**, 103702 (2011).
- [27] M. P. L. Sancho, J. M. L. Sancho, and J. Rubio, *I. Phys. F: Met. Phys.* **15**, 851 (1985).